Hydrogen Transfer by Graphene-NHC-Iridium Hybrid Catalysts Built through -OH Covalent Linkage.

Matías Blanco,[a] Patricia Álvarez,[a] Clara Blanco,[a] M. Victoria Jiménez,[b] Javier Fernández-Tornos,[b] Jesús J. Pérez-Torrente,[b] Luis A. Oro[b] and Rosa Menéndez*,[a]*

[a] Instituto Nacional del Carbón, CSIC, P.O. Box, 73, 33080-Oviedo, Spain. [b] Departamento de Química Inorgánica, Instituto de Síntesis Química y Catálisis Homogénea-ISQCH, Universidad de Zaragoza-C.S.I.C., 50009-Zaragoza, Spain.

ABSTRACT

Graphene oxide (GO) and thermally reduced graphene oxide (TRGO) were covalently modified with imidazolium salts through their hydroxyl surface groups. Selective reaction of the –OH groups with *p*-nitrophenylchloroformate produces labile intermediate organic carbonate functions which were used for the covalent anchoring of a hydroxy-functionalized imidazolium salt. The imidazolium-functionalized materials were used to prepare nanohybrid materials containing iridium N-heterocyclic carbene (NHC) type organometallic complexes by reaction with $[Ir(\mu\text{-}OMe)(cod)]_2$. Characterization of the graphene-based hybrid materials containing supported iridium N-heterocyclic carbene (NHC) complexes, **TRGO-1-Ir** and **GO-1-Ir**, through typical solid state characterization techniques, such as XPS or ICP-MS, allowed for the determination of 4.7 and 10.2 wt.% iridium loads, respectively. The graphene-supported iridium hybrid materials were active in the heterogeneous hydrogen-transfer reduction of cyclohexanone to cyclohexanol with 2-propanol/KOH as hydrogen source, being the thermally reduced material (**TRGO-1-Ir**) the catalyst with the best catalytic performance, even better than a related acetoxy-functionalized NHC iridium homogeneous catalyst, with an initial TOF of 11.500 h^{-1}. A good recyclability of the catalysts, without any loss of activity, and stability in air was observed.

1. Introduction

Graphenes are nowadays used in many research areas due to their unique properties, such as their excellent electronic behavior, their highly aromatic lattice which confers an exceptional mechanical strength, or their extraordinary chemical stability in most of the reaction media [1]. These properties make them outstanding supports to develop versatile matrixes for heterogeneous catalysts with enhanced activity [2]. Graphene oxide (GO) is usually obtained as an intermediate in the production of graphene by chemical methods (chemical oxidation of graphite), methodology which is considered nowadays as one of the most promising to produce graphenes at large scale, ensuring its availability [3,4]. Structurally, it can be considered as a graphene sheet decorated with oxygen functional groups at basal planes (i.e. epoxy and hydroxyl groups) and edges (carboxylic acids), and therefore with a variable amount of sp^3 hybridized carbon atoms disrupting the typical Csp^2 structure of graphene [5,6,7]. This distinctive structure can be chemically functionalized easily thereby expanding their field of application. In fact, functionalized graphene oxide has been extensively applied to areas such as composite materials, catalysis, optoelectronics, supercapacitors, memory devices and drug delivery [8,9,10]. Furthermore, the presence of oxygen functional groups on the aromatic scaffold of GO allows these sheets to mediate ionic and nonionic interactions with a wide range of molecules. Interestingly, GO by itself or in combination with other materials, show remarkable catalytic properties [11]. It is known that the presence of epoxy and hydroxyl functional groups on either side of the GO sheet imparts bifunctional properties that allow it to act as a structural node within metal-organic frameworks (MOFs), leading to improvements in catalytic activities by synergistic effects between the framework and the catalytically active center in the hybrid MOF.[12] In contrast, there are very few examples of supported molecular organometallic

compounds on functionalized graphene oxides with catalytic activity.[13] In these cases, a covalent linkage between the carbonaceous surface and the organometallic compound is highly desirable in order to reduce leaching. The common strategies described in the literature to achieve covalent functionalization exploit the carboxylic groups that decorate the edges of the GO sheets. This is the case of the esterification with nucleophiles (such as alcohols, amines or amino acids), directly in basic media,[14,15] or in the presence of $SOCl_2$,[16] oxalyl chloride,[17] or DCC (dicyclohexyl carbodiimide) [18]. Other oxygen-containing groups, different from carboxylic acids, have the advantage of being thermally more stable that the acids groups [19] and therefore are accessible within reduced graphene oxides (TRGO) in which the Csp^2 structure is partially restored. In this respect, the epoxy groups at the basal planes of the sheets have been used for functionalization via the amine groups of ionic liquids [20]. Hydroxyl groups have been scarcely explored for the functionalization of graphene derivatives [21] Most of them make use of difficult-handling and toxic siloxane derivatives and,[22] as far as authors are concerned, none of them has been used to support hybrid catalyst.

A number of highly efficient iridium−NHC (NHC = N-heterocyclic carbenes) catalysts active in hydrogen transfer catalysis have been reported [23] In particular, iridium(I) complexes with hemilabile O- and N-donor functionalized NHC ligands, having methoxy, dimethylamino, and pyridine as donor functions, are efficient catalyst precursors for transfer hydrogenation of unsaturated compounds using 2-propanol/KOH as hydrogen source [24] Interestingly, we have recently observed that iridium−NHC catalysts supported on carbon nanotubes through the carboxylic acids exhibit an enhanced hydrogen-transfer catalytic activity compared with related homogeneous systems [25].

The aim of this work is to prepare graphene-based hybrid catalysts by covalent functionalization of GO and TRGO through their surface –OH groups. The grafting of the GO/TRGO surface with NHC ligand precursors was achieved by reaction of hydroxo-functionalized imidazolium salts with intermediate carbonate species. The imidazolium-functionalized graphene materials were used to prepare hybrid materials containing iridium–NHC type organometallic complexes which were evaluated as heterogeneous catalysts for the hydrogen transfer reduction of cyclohexanone over several cycles in order to determine the recyclability and stability of the supported catalysts. In addition, the catalytic activity of a related homogeneous acetoxy-functionalized NHC iridium catalyst is described for comparative purposes.

2. Experimental

2.1.Materials

All chemicals, including powder graphite, were purchased from Aldrich, reagent or HPLC grade qualities were employed in all the experimental work. Solvents were distilled immediately prior to use from the appropriate drying agents or obtained from a Solvent Purification System (Innovative Technologies).

The GO utilized in this work was prepared applying a modified Hummers method to the commercial graphite as described previously [31]. TRGO was obtained from the correspondent graphite oxide by thermal treatment at 400ºC in an horizontal furnace, under a nitrogen flow of 50 mL min^{-1}. The residence time at the final temperature was 60 min [26]. The imidazolium salt [MeImH$(CH_2)_3$OH]Cl (**1**),[27] the starting organometallic compound [Ir(μ-OMe)(cod)]$_2$ [28] and

the acetoxy-NHC carbene complex [IrCl(cod)(MeIm$(CH_2)_3OCOCH_3$] (**Ir-ImidO**)[25] were prepared according to the literature procedures.

2.2. Characterization of Graphene Materials and Hybrid Catalysts

NMR spectra were recorded on a Bruker Advance 400 spectrometer at 400.16 MHz (^{1}H). NMR chemical shifts are reported in ppm relative to tetramethylsilane and referenced to partially deuterated solvent resonances. The catalytic reactions were analyzed on an Agilent 4890 D systems equipped with an HP-INNOWax capillary column (0.4 μm, 25 m x 0.2 mm i.d.) using mesitylene as internal standard. Thermogravimetric analyses (TGA) of the materials were performed in a TA SDT 2960 analyzer thermobalance. The procedure was as follow: 3 mg of sample were heated in the thermobalance at 10 ºC min^{-1} to 1000 ºC using a nitrogen flow of 200 mL min^{-1}. Transmission electron microscopy (TEM) spectra were carried out on a JEOL 2000 EX-II instrument operating at 160 kV. High-resolution images of transmission electron microscopy HRTEM of the samples were obtained using a JEOL JEM-2100F transmission electron microscope, equipped with a field-emission-gun (FEG) operating at 200 kV. Energy-dispersive X-ray spectroscopy (EDX) was used to verify the atomic composition of the catalyst. The samples were prepared by casting a few drops of 1 mg mL^{-1} ethanol suspensions of the materials over the carbon grids. To minimize exposure of the samples to the air, these were transferred to the lacey carbon grid into glovebox filled with ultrahigh-purity argon and from the glovebox to the TEM holder to minimize the time required to introduce them into the microscope. Elemental analyses were performed on a LECO-CHNS-932 micro-analyser with a LECO-VTF-900 furnace coupled to the micro-analyzer. The X-ray photoemission spectroscopy (XPS) spectra were performed in a SPECS system operating under a pressure of 10^{-7} Pa with a Mg Kα X-ray source. Functional groups in the graphene materials were quantified by

deconvolution of the high resolution C1s XPS peak in Gaussian and Lorentzian functions.[29] The binding energy profiles were deconvoluted as follows: undamaged structures of Csp^2-hybridized carbon (284.5 eV), damaged structures or Csp^3-hybridized carbons (285.5 eV), C-O groups (286.5 eV), C=O functional groups (287.7 eV) and COO groups at 288.7 eV. The amount of iridium present in the samples was determined by means of Inductively Coupled Plasma Mass Spectrometry (ICP-MS) in an Agilent 7700x instrument. The samples were digested following the method described elsewhere;[30] briefly, 30 mg of sample were treated with 5 mL of a mixture of concentrated nitric and hydrochloric acids (3:1 ratio) at 180 ºC for 3 h under microwave irradiation.

2.3. Functionalization of Graphene Materials with 1-(3-hydroxypropyl)-3-methyl-1H-imidazol-3-ium chloride (1)

Both type of graphenes (**GO** and **TRGO**) were functionalized with the imidazolium salt, 1-(3-hydroxypropyl)-3-methyl-1H-imidazol-3-ium chloride, [MeImH$(CH_2)_3$OH]Cl (**1**), following a two steps procedure. **GO** or **TRGO** (100 mg) were dispersed in 20 mL of dichloromethane (DCM). The dispersion was cooled to 0 ºC with an ice bath and then, *p*-nitrophenylchloroformate (3.0 g, 15 mmol) and triethylamine (2.1 mL, 15 mmol) were added under inert atmosphere. The mixture was stirred for 24 h and allowed to reach room temperature slowly. The resulting solids were filtered and washed three times with DCM (20 mL) and dried under vacuum for 2 h. In a second step, the imidazolium salt **1** (100 mg, 0.560 mmol) and a catalytic amount of triethylamine (0.2 mL) were added, under inert atmosphere, to dispersions of the graphene solids obtained in step 1 in tetrahydrofuran (THF) (15 mL), and refluxed for 24 h. The products were obtained by centrifugation/filtration, washed with THF (3 x 20 mL), DCM (3 x 20 mL), and ethanol (3 x 20 mL) and then, vacuum dried at 100 ºC in a preheated furnace until constant

weight. The obtained graphene samples were labeled as **GO-1** and **TRGO-1** depending on the parent material used in each case, **GO** or **TRGO**, respectively.

In another experiment, a dispersion of **GO** (100 mg) in THF (15 mL) was refluxed for 24 h. Centrifugation/filtration, washing with THF, DCM and ethanol, and vacuum drying at 100 ºC yielded **GO-Blank**.

2.4. Preparation of Hybrid Catalysts GO-1-Ir and TRGO-1-Ir

Imidazolium functionalized graphene materials, **GO-1** or **TRGO-1** (100 mg) were reacted with $[Ir(\mu\text{-}OMe)(cod)]_2$ (100 mg, 0.150 mmol) in THF (10 mL) under an argon atmosphere. The mixtures were refluxed for 2 days and then immersed into an ultrasonic bath for 30 min at room temperature. The resultant solids were recovered by centrifugation, washed with THF (5 x 10 mL) and diethyl ether (2 x 5 mL), and dried under vacuum to produce **GO-1-Ir** and **TRGO-1-Ir**.

General Procedure for Transfer Hydrogenation Catalysis. The catalytic transfer hydrogenation reactions were carried out under an argon atmosphere in thick glass reaction tubes fitted with a greaseless high-vacuum stopcock. In a typical experiment, the reactor was charged with a solution of cyclohexanone (0.52 mL, 5.0 mmol) in 2-propanol (4.5 mL), internal standard (mesitylene, 70 µL, 0.5 mmol), base (0.1 mL, 0.025 mmol of a KOH solution 0.24 M in 2-propanol) and the catalyst (0.005 mmol, 0.1 mol%). The weight of the supported catalysts used in each experiment was calculated according to the ICP measurements, assuming that all the iridium in the sample corresponds to active catalyst sites, 9.34 mg of **GO-1-Ir** (10.2 %wt of iridium) and 20.44 mg of **TRGO-1-Ir** (4.7 %wt of iridium). The resulting mixture was stirred at room temperature until complete solution of the homogeneous catalyst, $[IrCl(cod)(MeIm(CH_2)_3OCOCH_3]$ (**Ir-ImidO**),[25] or for 10 min. in the case of heterogeneous catalyst, and then placed in a thermostated oil bath at the required temperature, typically 80 ºC.

Conversions were determined by gas chromatography analysis under the following conditions: column temperature 35 ºC (2 min) to 220 ºC at 10 ºC/min, flow rate of 1 mL/min using ultrapure He as carrier gas.

Once the reaction was completed, the hybrid catalysts were recovered by centrifugation and washed with additional amounts of 2-propanol (3x10 mL). Several catalytic cycles were performed with these materials, under the same experimental conditions, without adding any fresh catalyst precursor. The last cycle was carried out without inert atmosphere.

3. Results and discussion

3.1. Functionalization of the -OH Groups in Graphene Oxide (GO) and Partially Reduced Graphene Oxides (TRGO).

GO was synthesized from commercial graphite by using the Hummers method. Following that procedure and, after sonication, water or dichloromethane homogeneous dispersions of monolayers of Csp^2 carbon atoms decorated with different oxygen-containing functional groups were obtained (see Supporting Information for details). As determined by XPS (Figure 1a), the functional groups observed include carboxylic acids (7.9 %), C=O (17.8 %) and C-O (29.6 %) groups. The presence of these functionalities at the basal planes of the sheet (alcohol or epoxy groups) or at the edges/holes (carboxylic acids, C=O groups) provides anchorage sites for the covalent linkage of different ligands and therefore, allowing for the preparation of hybrid materials. The amount of carbon atoms in a sp^2 hybridization (36.2 %) is however quite poor compared to that of graphene.[31] Nevertheless, thermal treatment of graphite oxide at 400ºC (**TRGO**, Figure 1b) led to the partial reconstruction of the Csp^2 structure (up to 71.4 %), due to

the elimination of the thermally unstable oxygen functional groups at this temperature (thermal reduction).

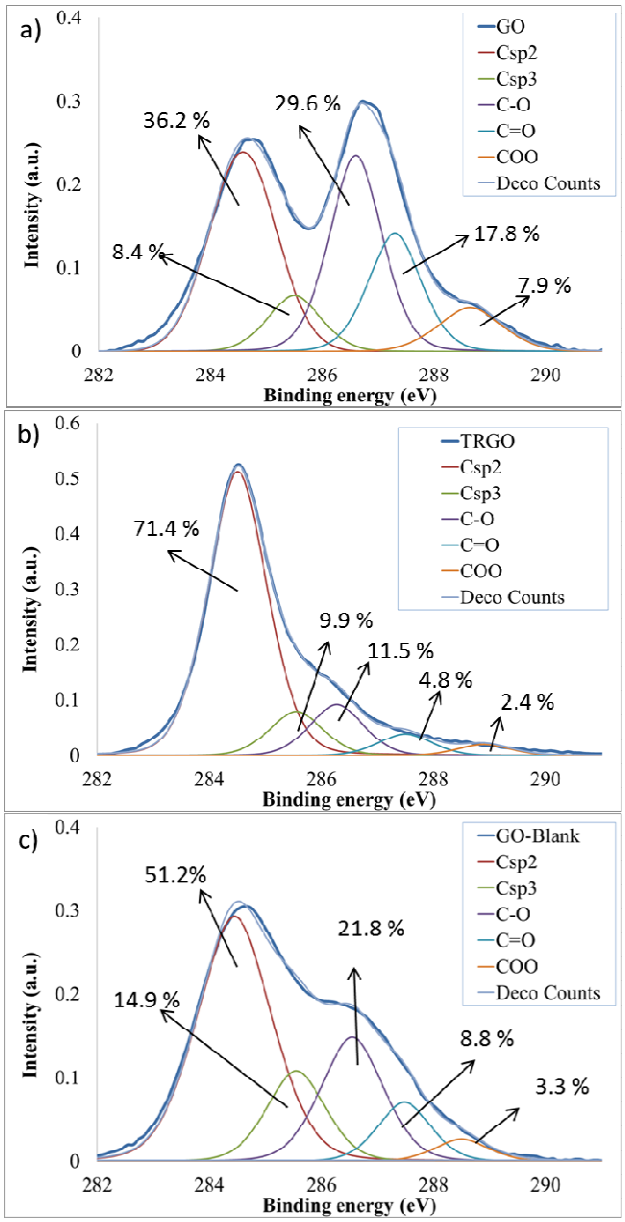

Figure 1. XPS C1s spectra and deconvoluted curves of: a) **GO**, b) **TRGO**, c) **GO-Blank**.

Despite the inherent loss of hydrophilicity, the thermally stable functional groups still present in **TRGO** are sufficient to form stable water and dichloromethane suspensions. Among them, the

most abundant oxygen-containing functions are the C-O groups (11.5 %), while the COO content (including acid groups being the less thermally stable)[19,32] is reduced down to 2.4 %. In view of the decrease in the acid groups content in this reduced material and, in order to broad the scope of the synthesis of organometallic supports, we have thought on the alternative functionalization of the carbonaceous materials through their OH groups, not only with thermally reduced graphene **TRGO**, but also with the parent **GO**.

The functionalization of the hydroxyl groups was achieved by means of a two-step procedure depicted in Figure 2. In a first step, **GO** and **TRGO** materials were reacted with *p*-nitrophenylchloroformate. This reactive is known to selectively react with "isolated" hydroxyl groups with the subsequent formation of the corresponding *p*-nitrophenyl carbonate esters [33,34,21] In a second step, treatment of the carbonates with the imidazolium salt [MeImH$(CH_2)_3$OH]Cl (**1**), which contains a nucleophile OH-ending group, in refluxing tetrahydrofuran for 24 h, resulted in the formation of new carbonate graphene derivatives, **GO-1** and **TRGO-1**, by *p*-nitrophenol displacement .

GO-1 and **TRGO-1** form relative stable suspensions in acetone (see Supporting Information), which allowed their characterization by NMR spectroscopy. Their ^{1}H NMR (acetone-d_6) spectra exhibit the typical set of signals for the imidazolium groups, at 7.41/7.35 ppm (H4 and H5) and 8.64 ppm (H2). Neither the corresponding signals of the nitrophenyl fragment nor the imidazolic -OH group were observed in the spectra. This is in agreement with a covalent linkage of **1** to the graphene derivative. The relatively few protons present in the graphene layered material were not observed in the ^{1}H NMR which is attributed to their poor relaxation, as it is proposed for related CNT-based materials [25] This fact also precludes the characterization of the samples by solid-state ^{13}C-CP MAS NMR spectroscopy (see Supporting Information).

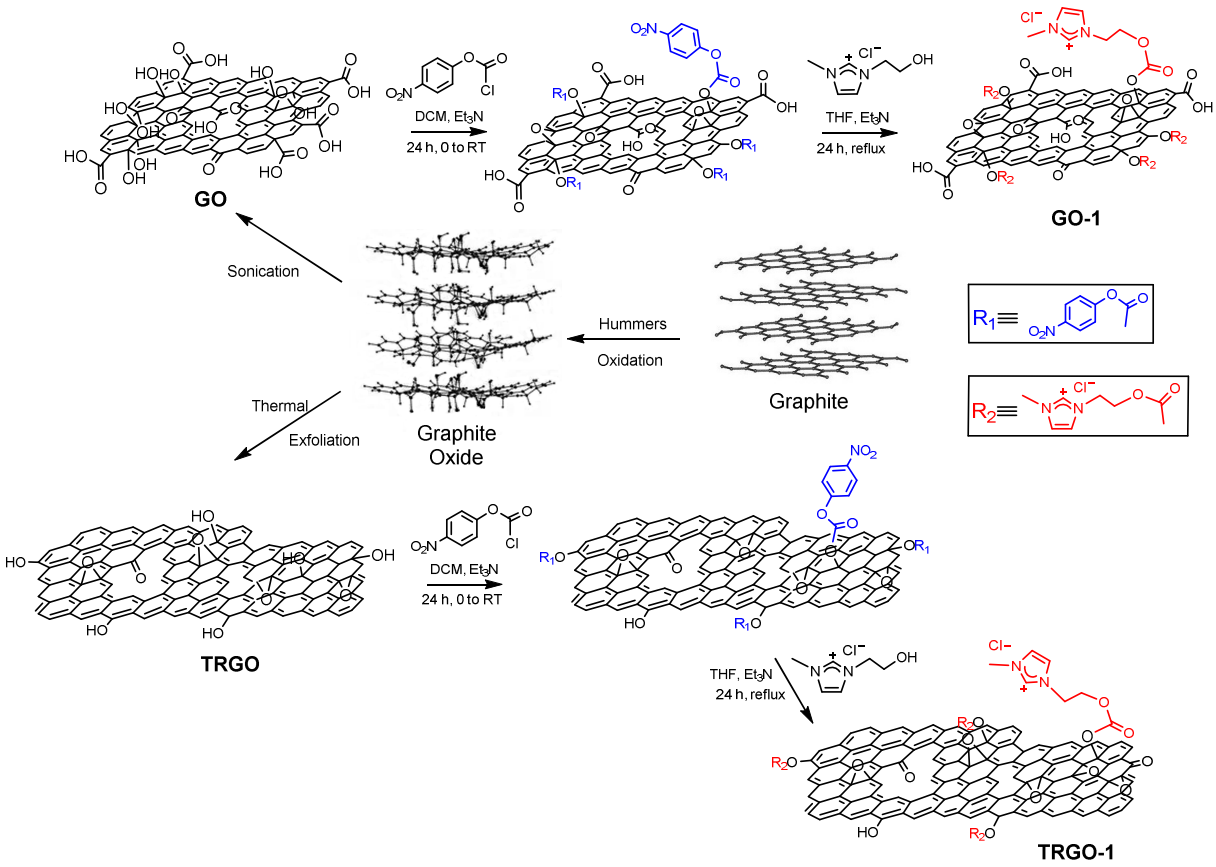

Figure 2. Covalent functionalization of the parent graphenes, **GO** and **TRGO**, with the imidazolium salt [MeImH$(CH_2)_3$OH]Cl (**1**).

It is well known that certain oxygen-containing functional groups of **GO** are readily decomposed even at low temperatures as a consequence of their low thermal stability [31]. Therefore, for comparative analytical purposes, the sample **GO-Blank** was prepared by refluxing suspensions of **GO** in boiling THF for 24 h. We have to take into account that **TRGO** was obtained at much higher temperature so the relative **TRGO-Blank** is irrelevant. Comparison of the TGA curves of **GO** and **GO-Blank** obtained under nitrogen (Figure 3) confirm the

significant lower weight loss of **GO-Blank** in the range below 110 ºC, which is related with the elimination of carboxylic acids and/or, in a lower extent, hydroxyl or epoxy groups located at the interior of the aromatic domains under the processing conditions [35]. This result was corroborated by XPS analysis of **GO-Blank** which shows a diminished amount of all types of C-O functional groups with a decrease of the acid groups down to 3.3% (Figure 1c). We can therefore conclude that a large amount of the carboxylic acids in **GO** were lost under the reaction conditions applied for the preparation of **GO-1**, and not by reaction with the imidazolium ligand, therefore confirming the highly selective imidazolium anchoring to the –OH functionalities on the graphene surface.

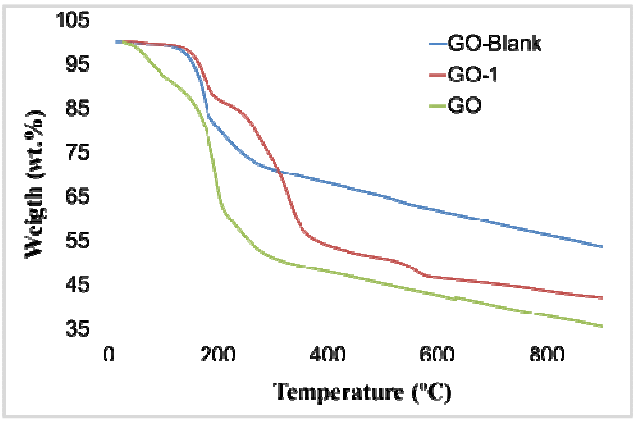

Figure 3. Thermogravimetric analysis profiles of **GO**, **GO-1** and **GO-Blank**.

The imidazolium functionalization of **GO-1** and **TRGO-1** was further confirmed by elemental analysis (Table 1) which shows an increase in the nitrogen content with respect to the parent **GO** and **TRGO**, from ≈ 0.1 wt.% in the parent samples up to 6.9 and 1.4 wt.% for **GO-1** and **TRGO-1**, respectively, which is consistent with the attachment of the imidazolium ligand on the graphene sheets. The lower amount of nitrogen in **TRGO-1** compared to that of **GO-1** is

obviously related with the lower amount of C-O groups in the parent thermally reduced sample, which restricts its capacity to bond imidazolium salt. The increment of the atomic nitrogen content in these samples calculated by XPS (Table 1) is also consistent with the above conclusions. Additionally, and as expected, chlorine atoms were also detected by XPS in a half ratio of the nitrogen content.

Table 1. Elemental analysis and XPS data of parent graphenes (**GO** and **TRGO)** and imidazolium functionalized graphenes (**GO-1** and **TRGO-1)**.

Sample	**Elemental Analysis (wt.%)**				**XPS (%)**	
	C	*H*	*N*	*O*	*N*	*Cl*
GO	49.1	2.4	0.1	48.4	0.0	0.0
TRGO	74.1	0.6	0.0	25.3	0.0	0.0
GO-1	51.8	3.4	6.9	37.9	5.6	2.5
TRGO-1	76.8	1.4	1.4	20.3	1.4	0.6

Detailed analysis of the high-resolution XPS C1s peaks of **GO-1** and **TRGO-1** (Figure 4, a and b, respectively) show the appearance of the typical band of the C-N bonds which is not present neither in the parent materials nor in **GO-Blank**. Unfortunately, this band lies in between the Csp^3 and C-O bands, which prevent their quantification. The increment in the intensity of the COO band in **TRGO-1** and **GO-1** with respect the parent **TRGO** and the thermally treated **GO-Blank** (to discriminate the effect of the temperature in the elimination of functional groups) is mainly ascribed to the new carbonate groups formed in the functionalization process.

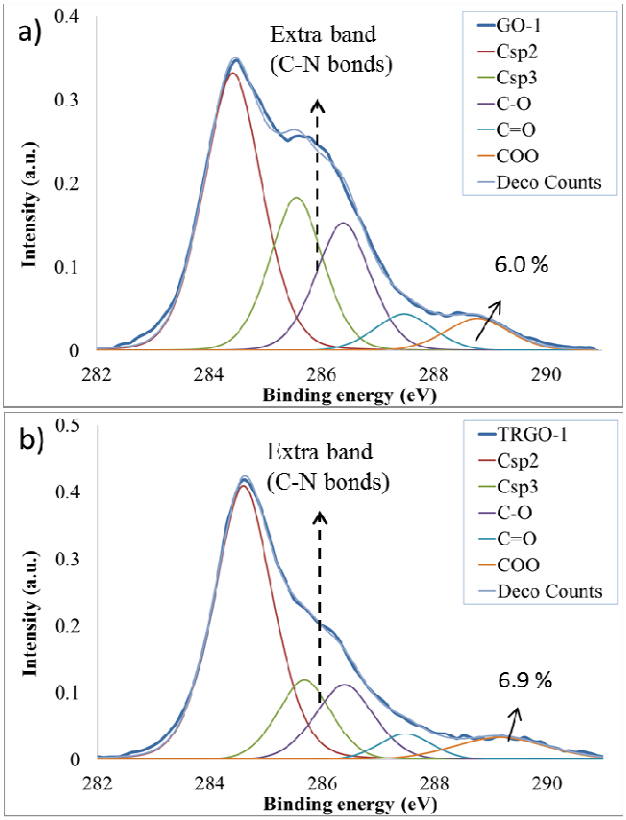

Figure 4. XPS C1s spectra and deconvoluted curves of imidazolium functionalized graphenes: a) **GO-1**, b) **TRGO-1**.

TEM images of **GO-1** and **TRGO-1** (Figure 5, c and d) are similar to those of the corresponding precursors, **GO** and **TRGO** (Figure 5, a and b). Also, the thermally reduced samples show the expected fluffy appearance what indicates that the functionalization do not produce any damage in the graphene layers.

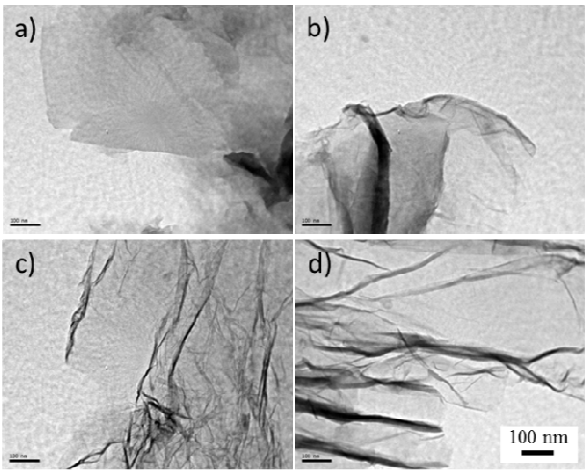

Figure 5. TEM images of a) **GO**, b) **TRGO**, c) **GO-1**, and d) **TRGO-1**.

3.2. Synthesis and characterization of hybrid graphene/iridium catalysts.

The hybrid catalysts containing supported iridium N-heterocyclic carbene (NHC) complexes, **GO-1-Ir** and **TRGO-1-Ir**, were prepared by reaction of the methoxo iridium(I) dimer compound $[Ir(\mu\text{-}OMe)(cod)]_2$ (cod = 1,5-cyclooctadiene) with the imidazolium functionalized graphenes, **GO-1** and **TRGO-1**, as depicted in Figure 6. Insoluble materials were obtained in both cases, probably as a consequence of the increment in the molecular weight of the samples, which prevent their characterization in solution by NMR. Evidence for the successful anchoring of the NHC-iridium complexes on the graphene oxide sheets was obtained from XPS spectroscopy. For comparative purposes the materials **GO-Ir** and **TRGO-Ir** were prepared by reaction of the unfunctionalized **GO** and **TRGO** (lacking the supported imidazolium ligand) with $[Ir(\mu\text{-}OMe)(cod)]_2$.

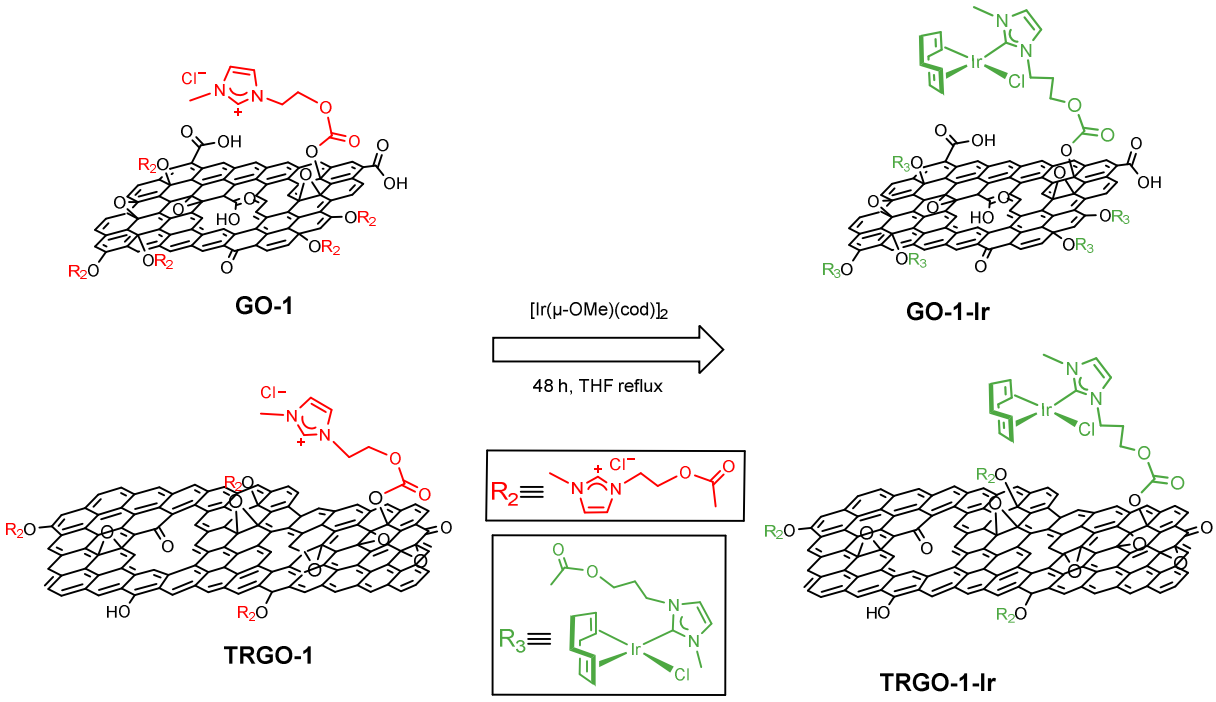

Figure 6. Synthesis of hybrid graphene/Ir-NHC materials.

The high-resolution Ir4f XPS peak obtained for all iridium samples (Figure 7) shows the two characteristic peaks of the iridium ($Ir4f_{7/2}$ and $Ir4f_{5/2}$). Both peaks were centered at 62.4 and 65.6 eV for the functionalized materials containing the NHC linkers, **GO-1-Ir** and **TRGO-1-Ir**. These values compare well with those observed for related iridium(I) compounds,[36] or nanotube-supported iridium-NHC hybrid materials recently describe by us [25]. However, in **GO-Ir** and **TRGO-Ir**, lacking NHC linkers, the maxima are shifted towards higher binding energies, 63.0 and 66.1 eV, respectively. This suggests that in the absence of the imidazolium ligand **1** the iridium centers could be in an upper oxidation state (i.e. iridium oxide) [37] or alternatively taking part of very different iridium species (i.e, iridium nanoparticles,[38] carboxylate-complexes,[39] clusters,[40] etc.).

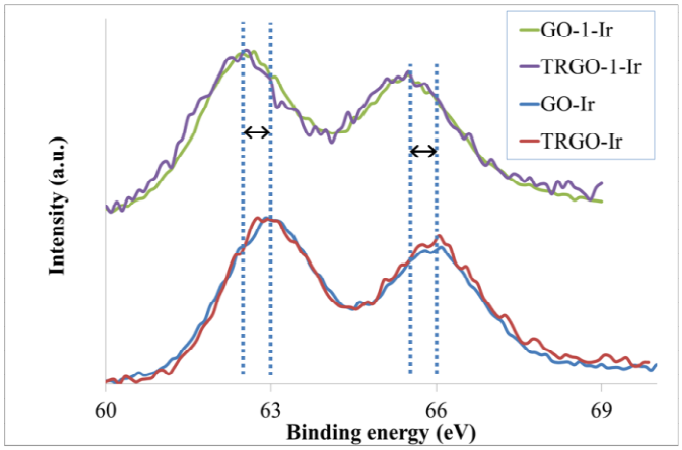

Figure 7. XPS spectra for the Ir4f core level of the graphene-based Ir hybrid catalysts.

The amount of iridium in the hybrid catalysts, determined by means of ICP-MS measurements, was 10.2 wt.% for **GO-1-Ir** and 4.7 wt.% for **TRGO-1-Ir**. For the samples without imidazolium ligands, **GO-Ir** and **TRGO-Ir**, the amount of iridium loaded was higher, 19.9 and 6.0 wt.%, respectively, most probably as a result of the different attachment mode of the iridium to the oxygen functional groups of the graphene materials.

HRTEM images obtained for **GO-1-Ir** (Figure 8) showed the presence of supported iridium species homogeneously distributed at the surface of the graphene sheets, which was also confirmed by EDX spectroscopy (see Supporting Information). Iridium species with diameters as lower as 0.17-0.27 nm and greater (1.2-1.4 nm and even larger) were observed. According to other authors, these findings could be attributed to the presence of molecular iridium complexes anchored on the surface (lower diameters) together with iridium clusters or nanoparticles possibly formed by beam damage when measuring that cause iridium migration. These electron-dense regions have also been observed in the characterization of related molecular iridium analogues [25].

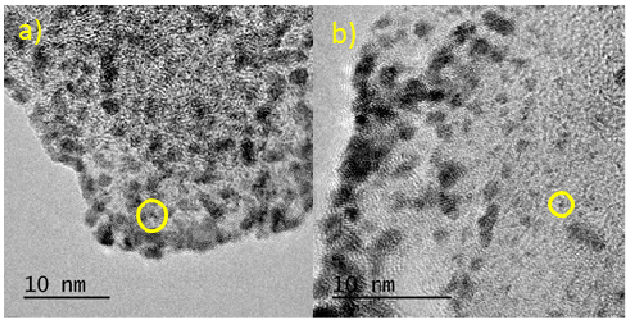

Figure 8. HRTEM images of a) **GO-1-Ir** and b) **TRGO-1-Ir**.

Although there is no direct evidence of the covalent coordination of the IrCl(cod) metal fragment, considering the above results, it is suggested that the functionalization of the nanomaterials was achieved through the carbene atom of the heterocycle moiety in a similar way to that of the Ir-NHC homogeneous catalysts.

3.3. Hydrogen-Transfer Catalytic Activity.

The supported organometalllic complexes **GO-1-Ir** and **TRGO-1-Ir** graphene materials were therefore tested as catalysts for the hydrogen transfer reduction of cyclohexanone to cyclohexanol (Equation 1) using 2-propanol both as hydrogen source and as a non-toxic solvent with a moderate boiling point. The catalytic transfer hydrogenation of several unsaturated substrates, including cyclohexanone, under homogeneous conditions were previously tested and optimized for a set of O-functionalized NHC iridium(I) related complexes such as [IrBr(cod)(MeIm(2-methoxybenzyl))] [24] Standard catalyst loads of 0.1 mol %, with 0.5 mol % of KOH as co-catalyst, and 80 ºC were routinely employed (Equation 1). The supported catalysts prepared without imidazolium ligand, **GO-Ir** and **TRGO-Ir**, and the related molecular acetoxy-functionalized NHC complex [IrCl(cod)(MeIm$(CH_2)_3OCOCH_3$] (**Ir-ImidO**) [25] were also

evaluated for comparative purposes. It is noteworthy that all the graphene materials without iridium did not show any catalytic activity.

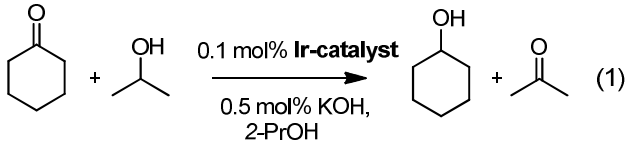

Reaction profiles obtained for heterogeneous and homogeneous catalysts are shown in Figure 9. The relevant reaction parameters, including the reaction times required to reach 90% conversion and the turnover frequencies (TOF), for all the examined catalysts are summarized in Table 2. As can be observed in the conversion vs time reaction profiles (Figure 9), no induction period was detected, as cyclohexanone reduction was immediately observed after thermal equilibration of the reactant mixture. The reaction profiles illustrate the outstanding catalytic activity of the graphene-supported iridium-NHC hybrid materials, **GO-1-Ir** and **TRGO-1-Ir**, compared with those materials lacking a NHC linker between the carbon material and iridium, **GO-Ir** and **TRGO-Ir**. In fact, the later materials became deactivated after 3 hours reaching less than 20% conversion. The hybrid material **TRGO-1-Ir** is the catalyst with the best catalytic performance, even better than the homogeneous acetoxy-functionalized NHC catalyst [IrCl(cod)(MeIm$(CH_2)_3OCOCH_3$] (**Ir-ImidO**).

The reaction time required to reach 90% conversion (as determined by GC using mesitylene as internal standard) for **TRGO-1-Ir** was 150 min, much shorter than that observed for the homogeneous catalyst [IrCl(cod)(MeIm$(CH_2)_3OCOCH_3$] (**Ir-ImidO**) of 200 min, and definitively much better than the 760 min required for the **GO-1-Ir** material. These results point out to an influence of the graphene support in the enhancement of the catalytic activity when compare with the homogeneous system. On the other hand, the superior catalytic activity of

TRGO-1-Ir is a consequence of the structural features of the reduced graphene material. Most probably, the higher structural Csp^2 area of this thermally reduced type of graphene **TRGO** compared with the parent **GO** sample has a positive influence. The poor catalytic performance of **GO-1-Ir** could be related with the presence of a great variety of oxygen functional groups in this sample. This other groups (i.e. carboxylic acids) could also react with the iridium precursor in a competitive way leading to iridium carboxylate or alkoxide complexes with much lower catalytic activity than the supported iridium NHC species.

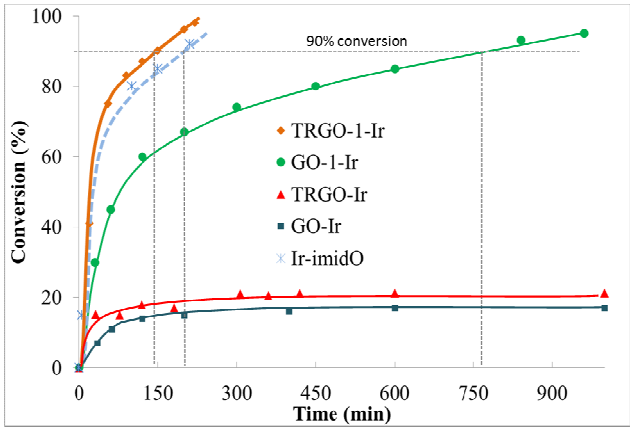

Figure 9. Reaction profiles for transfer hydrogenation of cyclohexanone by homogeneous and heterogeneous catalysts.

Successful recycling studies were carried out with both graphene-supported iridium-NHC hybrid catalysts **GO-1-Ir** and **TRGO-1-Ir**. The catalyst without NHC linkers, **GO-Ir** and **TRGO-Ir**, could not be re-cycled (Figure 10). The recycling procedure simply requires filtration, washing of the catalysts with fresh 2-propanol (4 x 5 mL), and addition of further cyclohexanone/KOH/i-PrOH. The process was repeated four times in protected atmosphere, and in the fifth run, the catalytic reactions were conducted in air. The results of cyclohexanone conversion after each catalytic run, with reaction times of 2.5 h for **TRGO-1-Ir** and 12.5 h for

GO-1-Ir, are depicted in Figure 10. Both graphene-supported iridium-NHC hybrid catalysts exhibited comparable conversions in the successive experiments, even for the fifth cycle under no protected atmosphere. This behavior contrast with the impossibility to recycle the acetoxy-functionalized iridium-NHC homogeneous catalysts (**Ir-ImidO**) due to its air-sensitivity.

Table 2. Catalytic Hydrogen Transfer from 2-Propanol to Cyclohexanone with graphene/Ir-NHC and graphene/Ir hybrid catalysts, and related acetoxy-functionalized NHC-Ir homogeneous catalyst (Ir-ImidO).[a,b]

Catalyst	**Time (min)[c]**	**TON**	**TOF_0, h^{-1}**	**TOF_{90}, h^{-1}**
GO-1-Ir	760	947	11364	75
TRGO-1-Ir	150	964	11568	385
GO-Ir	-	147	441	-
TRGO-Ir	-	203	609	-
Ir-ImidO	200	941	11124	282

[a] Reaction conditions: catalyst/substrate/KOH ratio of 1/1000/5, 0.1 mol% of catalyst in 5 mL 2-propanol (5 mL) at 80 °C. [b] The reactions were monitored by GC using mesitylene as internal standard. [c] Reaction time at 90% of conversion.

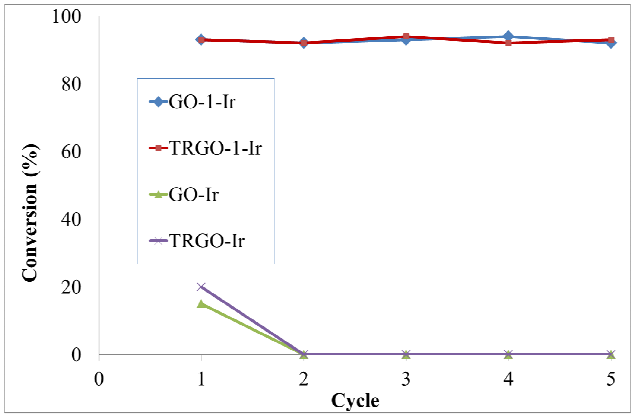

Figure 10. Recyclability of graphene-supported iridium heterogeneous catalysts.

4. Conclusions

We have demonstrated that graphene oxides and partially reduced graphene oxides can be conveniently functionalized through the hydroxyl surface groups. Covalent anchoring of a hidroxy-functionalized imidazolium salt was achieved through labile intermediate organic carbonate functions prepared by the selective reaction of the -OH groups with *p*-nitrophenylchloroformate. The imidazolium functionalized graphene materials were used to prepare hybrid materials containing supported iridium N-heterocyclic carbene (NHC) complexes covalently bonded through carbonate functions.

The hybrid graphene/iridium-NHC materials were active catalysts in the hydrogen transfer reduction of cyclohexanone to cyclohexanol using 2-propanol as hydrogen source. Interestingly, a superior catalytic performance was achieved for the partially reduced graphene-based material. This heterogeneous catalyst is slightly more active than a related acetoxy-functionalized NHC iridium homogeneous catalyst. The enhanced catalytic activity most probably is due to the positive effect of Csp^2 structure in partially reduced graphenes. However, both types of catalysts present very similar reaction profiles thus suggesting a similar operating mechanism. In contrast, the presence of remaining oxygen functional groups as competitive sites for the anchoring of

poorly active iridium complexes seems to be the reason for the low catalytic performance of hybrid catalyst based on graphene oxide lacking NHC-linkers.

It was also demonstrated that the graphene-based heterogeneous hybrid catalysts remained stable through successive catalytic runs. The supported catalyst can be reused in five consecutive cycles without any loss of activity, even under an air atmosphere.

EXPERIMENTAL SECTION

ASSOCIATED CONTENT

Supporting Information. Characterization data of parent and functionalized **GOs** and **TRGOs**. This material is available free of charge via the Internet at http://pubs.acs.org.

Author Contributions

The manuscript was written through contributions of all authors. All authors have given approval to the final version of the manuscript.

ACKNOWLEDGMENT

The authors thank MICINN (Projects Consolider Ingenio 2010 CSD2009-00050 and CTQ 2010-15221), and the Diputación General de Aragón (E07) for their financial support. Dr. P. A. thanks MICINN for a Ramón y Cajal contract. J. F-T. and M. B. acknowledge their fellowships from MICINN and MECD (AP2010-0025).

References

[1] (a) Mao H Y, Laurent S, Chen W, Akhavan O, Imani M, Ashkarran A A, Mahmoudi M. *Chem. Rev*. **2013**, *113*, 3407−3424. (b) Haddon, R. C. *Acc. Chem. Res*. **2013**, *46*, 1–3. (c) Park, S.; Ruoff, R. S. *Nat. Nanotechnol*. **2009**, *4*, 217–224.

[2] (a) Dai, L. *Acc. Chem. Res.* **2013**, *46*, 31–42. (b) Park, J.; Yan, M. *Acc. Chem. Res.* **2013**, *46*, 181–189. (c) Schaetz, A.; Zeltner, M.; Stark, W. J. *ACS Catal.* **2012**, *2*, 1267−1284.

[3] Marcano, D. C.; Kosynkin, D. V.; Berlin, J. M.; Sinitskii, A.; Sun, Z.; Slesarev A.; Alemany, L. B.; Lu, W.; Tour, J. M. *ACS Nano* **2010**, *4*, 4806–4814.

[4] Zhao, J.; Pei, S.; Ren, W.; Gao, L.; Cheng, H. ACS Nano **2010**, *4*, 5245–5252.

[5] Lerf, A.; He, H.; Forster, M.; Klinowski J. *J. Phys. Chem. B* **1998**, *102*, 4477–4482.

[6] Szabo, T.; Berkesi, O.; Forgo, P.; Josepovits, K.; Sanakis, Y.; Petridis, D.; Dékány, I. *Chem. Mater*. **2006**, *18*, 2740–2749.

[7] Dreyer, D. R.; Park, S.; Bielawski, C. W.; Ruoff, R. S. *Chem. Soc. Rev.* **2010**, *39*, 228–240.

[8] Ramanathan, T.; Abdala, A. A.; Stankovich, S.; Dikin, D. A.; Herrera-Alonso, M.; Piner, R. D.; Adamson, D. H.; Schniepp, H. C.; Chen, X.; Ruoff, R. S.; Nguyen, S. T.; Aksay, I. A.; Prud'Homme, R. K.; Brinson, L. C. *Nat. Nanotechnol.* **2008**, *3*, 327–331.

[9] González, Z.; Botas, C.; Álvarez, P.; Roldán, S.; Blanco, C.; Santamaría, R.; Granda, M.; Menéndez. R. *Carbon* **2012**, *50*, 828–834.

[10] Krishnamoorthy, K.; Mohan, R.; Kim, S. -J. *Appl. Phys. Lett.* **2011**, *98*, 244101.

[11] (a) Navalon, S.; Dhakshinamoorthy, A.; Alvaro, M.; Garcia, H. *Chem. Rev.* **2014**, 114, 6179–6212. (b) Shi, P.; Dai, X.; Zheng, H.; Li, D.; Yao, D.; Yao, W.; Hu, C. *Chem. Eng. J.* **2014**, *240*, 264–270. (c) Su, C.; Loh, K. P. *Acc. Chem. Res.* **2013**, *46*, 2275–2285. (d) Pyun, J. *Angew. Chem. Int. Ed.* **2011**, *50*, 46–48.

[12] Jahan, M.; Bao, Q. L.; Loh, K. P. *J. Am. Chem. Soc.* **2012**, *134*, 6707–6713.

[13] (a) Sabater, S.; Mata, J. A.; Peris, E. *ACS Catal.* **2014**, *4*, 2038−2047. (b) Zhao, Q.; Li, Y.; Liu, R.; Chen, A.; Zhang, G.; Zhang, F.; Fan, X. *J. Mater. Chem. A* **2013**, *1*, 15039–15045. (c) Stankovich, S.; Piner, R. D.; Chen, X.; Wu, N.; Nguyen, S. T.; Ruoff, R. S. *J. Mater. Chem.* **2006**, *16*, 155–158. (d) Stankovich, S.; Piner, R. D.; Nguyen, S. T.; Ruoff, R. S. *Carbon* **2006**, *44*, 3342–3347. (e) Stankovich, S.; Dikin, D. A.; Dommett, G. H. B.; Kohlhaas, K. M.; Zimney, E. J. *Nature* **2006**, *442*, 282–286. (f) Viculis, L. M.; Mack, J. J.; Mayer, O. M.; Hahn, H. T.; Kaner, R. B. *J. Mater. Chem.* **2005**, *15*, 974–978.

[14] Kakran, M.; Sahoo, G. N.; Bao, H.; Pan, Y.; Li, L. *Curr. Med. Chem.* **2011**, *18*, 4503–4512.

[15] Mallakpour, S.; Abdolmaleki, A.; Borandeh, S. *Appl. Surf. Sci.* **2014**, *307*, 533–542.

[16] Xu, C.; Wang, X.; Wang, J.; Hu, H.; Wan, L. *Chem. Phys. Lett.* **2010**, *498*, 162–167.

[17] Karousis, N.; Economopoulos, S. P.; Sarantopoulou, E.; Tagmatarchis, N. *Carbon* **2010**, 48, 854–860.

[18] (a) Liu, Y.; Yu, D.; Zeng, C.; Miao, Z.; Dai, L. *Langmuir* **2010**, *26*, 6158–6160. (b) Shen, J.; Shi, M.; Yan, B.; Ma, H.; Li, N.; Hu, Y.; Ye, M. *Colloid Surface B: Biointerfaces* **2010**, *81*, 434438.

[19] Figueiredo, J. L. *Carbon* **1999**, *37*, 1379–1389.

[20] Yang, H.; Shan, C.; Li, F.; Han, D.; Zhang, Q.; Niu, L. *Chem. Comum.* **2009**, 3880–3882.

[21] Shi, J.; Wang, L.; Zhang, J.; Ma, R.; Gao, J.; Liu, Y.; Zhang, C.; Zhang, Z. *Biomaterials* **2014**, *35*, 5847–5861.

[22] Chen, L.; Chai, S.; Liu, K.; Ning, N.; Gao, J.; Liu, Q.; Chen, F.; Fu, Q. *ACS Appl. Mater. Interfaces* **2012**, *4*, 4398–4404.

[23] (a) Modugno, G.; Monney, A.; Bonchio, M.; Albrecht, M.; Carraro, M. *Eur. J. Inorg. Chem.* **2014**, 2356–2360. (b) Gülcemal, S.; Gökçe, A. G.; Çetinkaya, B. *Inorg. Chem.* **2013**, *52*, 10601–10609. (c) Azua, A.; Mata, J. A.; Peris, E.; Lamaty, F.; Martínez, J.; Colacino, E. *Organometallics* **2012**, *31*, 3911–3919. (d) Gierz, V.; Urbanaite, A.; Seyboldt, A.; Kunz, D. *Organometallics* **2012**, *31*, 7532–7538. (e) Newman, P. D.; Cavell, K. J.; Hallett, A. J.; Kariuki, B. M. *Dalton Trans.* **2011**, *40*, 8807–8813. (f) Diez, C.; Nagel, U. *App. Organomet. Chem.* **2010**, *24*, 509–516. (g) Pontes da Costa, A.; Viciano, M.; Sanaú, M.; Merino, S.; Tejeda, J.; Peris, E.; Royo, B. *Organometallics* **2008**, *27*, 1305–1309. (h) Hahn, F. E.; Holtgrewe, C.; Pape, T.; Martin, M.; Sola, E.; Oro, L. A. *Organometallics* **2005**, *24*, 2203–2209. (i) Mas-Marzá, E.; Poyatos, M.; Sanaú, M.; Peris, E. *Organometallics* **2004**, *23*, 323–325. (j) Albrecht, M.; Crabtree, R. H.; Mata, J. A.; Peris, E. *Chem. Commun.* **2002**, 32–33. (k) Hillier, A. C.; Lee, H. M.; Stevens, E. D.; Nolan, S. P. *Organometallics* **2001**, *20*, 4246–4252.

[24] (a) Jiménez, M. V.; Fernández-Tornos, J.; Pérez-Torrente, J. J.; Modrego, F. J.; Winterle, S.; Cunchillos, C.; Lahoz, F. J.; Oro, L. A. *Organometallics* **2011**, *30*, 5493–5508. (b) Türkmen, H.; Pape, T.; Hahn, F. E.; Çetinkaya, B. *Eur. J. Inorg. Chem.* **2008**, 54185423.

[25] Blanco, M.; Álvarez, P.; Blanco, C. Jiménez, M. V.; Fernández-Tornos, J.; Pérez-Torrente, J. J.; Oro, L. A.; Menéndez, R. *ACS. Catal.* **2013**, *3*, 1307–1317.

[26] Botas, C.; Álvarez, P.; Blanco, C.; Santamaría, R.; Granda, Gutiérrez, M. D.; F. Rodríguez-Reinoso, F.; Menéndez, R. *Carbon* **2013**, *52*, 476–485.

[27] Bekhouche, M.; Blum, L. J.; Doumèche, B. *ChemCatChem* **2011**, *3*, 875–882.

[28] Usón, R.; Oro, L. A.; Cabeza, J. A. *Inorg. Synth.* **1985**, *23*, 126–127.

[29] Sherwood, P. M. A. In *Practical Surface Analysis in Auger and X-ray Photoelectron Spectroscopy*; Briggs, D., Seah, M. P., Eds.; Wiley: New York, 1990, Vol. 1, pp. 574.

[30] Elgrabli, D.; Floriani, M.; Abella-Gallar, S.; Meunier, L.; Gamez, C.; Delalain, P.; Rogerieux, F.; Boczkowski, J.; Lacroix, G. *Part. Fibre Toxicol.* **2008**, *5*, 20–33.

[31] (a) Botas, C.; Álvarez, P.; Blanco, P.; Granda, M.; Blanco, C.; Santamaria, R.; Romasanta, L.J.; Verdejo, R.; López-Manchado, M.A.; Menéndez, R. *Carbon* **2013**, *65*, 16–164. (b) Botas, C.; Álvarez, P.; Blanco, C.; Santamaría, R.; Granda, M.; Ares, P.; Rodríguez-Reinoso, F.; Menéndez, R..*Carbon* **2012**, *50*, 275-282.

[32] Chen, D.; Feng, H.; Li, J. *Chem. Rev.* **2012**, *112*, 6027–6053.

[33] Letsinger, R. L.; Ogilvie, K. K. *J. Org. Chem.* **1967**, *32*, 296–300.

[34] Oh, J. K.; Drumright, R.; Siegwart, D. J.; Matyjaszewski K. *Prog. Polym. Sci.* **2008**, *33*, 448–477.

[35] Gao, X.; Jang, J.; Nagase, S. *J. Phys Chem. C* **2010**, *114*, 832–842.

[36] Crotti, C.; Farnetti, E.; Filipuzzi, S.; Stener, M.; Zangrando. E.; Moras, P. *Dalton Trans.* **2007**, 133–142.

[37] Lee, W. H.; Kim, H. *Catal. Commun.* **2011**, *12*, 408–411.

[38] Zahmakiran, M. *Dalton Trans.* **2012**, *41*, 12690–12696.

[39] (a) Giordano, R.; Serp, P.; Kalck, P.; Kihn, Y.; Schreiber, J.; Marhic, C.: Duvail, J. -L. *Eur. J. Inorg. Chem.* **2003**, 610–617. (b) Díaz-Auñón, J. A.; Román-Martínez, M. C.; Salinas-Martínez de Lecea, C. *J. Mol. Cat. A: Chemical* **2001**, *170*, 81–93.

[40] (a) Mungse, H. P.; Verma, S.; Kumar, N.; Sain, B.; Khatri, O. P. *J. Mater. Chem.* **2012**, *22*, 5427–5433. (b) Fritsch. A.; Légaré, P. *Surf. Sci*. **1984**, *145*, L517–L523.

For the Table of Contents

Graphene-NHC-Ir Hybrid Catalysts